

# Noncontact Human Force Capturing based on Surface Hardness Measurement

Masahiro Fujiwara\* and Hiroyuki Shinoda†  
The University of Tokyo

## ABSTRACT

In this paper, we propose a remote grip force sensing method based on skin surface hardness measurement. The measurement system is composed of an airborne ultrasound phased array and a laser displacement sensor. The surface hardness distribution of a human hand is estimated by optically measured surface vibration amplitude induced by the ultrasound radiation pressure. The real-time grip force is estimated using the relationship between the hand surface compliance and the grip force which is obtained experimentally in advance. The feasibility of grip force estimation is confirmed for a gripping hand keeping a constant posture.

**KEYWORDS:** Force measurement, hardness measurement, acoustic radiation pressure, biomechanics.

**INDEX TERMS:** H.5.2 [Information Interfaces and Presentation] User Interfaces—Haptic I/O; J.3 [Computer Applications]: Life and Medical Sciences—Medical Information Systems

## 1 INTRODUCTION

Muscle force is one of the most essential parameters to describe human actuation activities. Although videos or visual motion capture systems are convenient and powerful tools to record human skillful motions, they lack force information which is often more important than the motion trajectory for obtaining the knacks of skills. Figure 1 explains the difficulty of force estimation from videos. The isotonic contraction maintains the contraction tension while the muscle fiber length changes [1]. This isotonic contraction can accompany skeletal movements including a concentric motion and an eccentric motion. The isometric contraction maintains a constant posture by balancing the muscle tension with the external force. These two contractions are mixed in general movements, which are difficult to be resolved by video images.

In order to record force information in human activities, a lot of methods have been proposed. A straightforward method is to mount a force sensor on the human finger or the object surface. Electromyography (EMG) is another approach that needs no devices on the finger contacting with an object, although electrodes are required on the other skin surface [2]-[7]. These studies have revealed correlations among the EMG signal, the degree of muscle contraction, and muscle fiber conduction velocity.

---

Address: Faculty of Engineering Bldg. 2, 7-3-1 Hongo, Bunkyo-ku, Tokyo 113-8656, Japan.  
\*e-mail: fujiwara@alab.t.u-tokyo.ac.jp  
†e-mail: shino@alab.t.u-tokyo.ac.jp

IEEE World Haptics Conference 2013  
14-18 April, Daejeon, Korea  
978-1-4799-0088-6/13/\$31.00 ©2013 IEEE

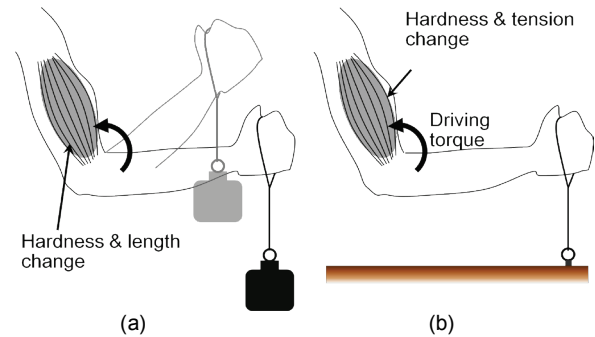


Figure 1. Muscle hardness change by (a) isotonic contraction and (b) isometric contraction.

These methods require mounted sensors or electrodes on the skin that sometimes constrain the human activity and they can be applied to only fixed and local areas on the human body practically. The requirement that the human should wear some special device in advance can be a fatal inconvenience in human-computer interface (HCI) applications.

In this paper, we propose a remote force estimation method by non-contact measurement of the skin surface hardness. Last year we showed that remote hardness sensing is possible by measuring the surface vibration caused by radiation pressure of airborne ultrasound [8]. By scanning the pressurization position with an ultrasound phased array, we can obtain a surface compliance distribution. We apply this method for evaluating grip forces.

It is known that contracted muscle hardness increases with the generated force regardless of presence or absence of the positional constraint. It has been confirmed that the muscle hardness is proportional to the muscle tension over a wide range [9]. Therefore the muscle hardness can be an index of the force generated by the muscle contraction. The experimental results of this paper show we can detect a grip force change caused by static isometric contraction without attaching any devices on the hand or the gripped object.

As for contact methods of hardness measurement, various methods for a soft tissue have been proposed [10]-[13]. Ultrasound measurement of hardness distribution is also reported in [11]-[13]. These methods are limited to contact measurement or measuring in water. The proposed non-contact system has a wide application fields from scientific researches of motion analysis to HCI. In HCI applications, we can send our commands to the system quickly and precisely through human force generation.

In the following sections, the feasibility of grip force estimation is examined for a gripping hand keeping a constant posture. Although the grip force measurement is a successful example, we have to notice that the surface hardness cannot quantify all the muscle forces deterministically. For an antagonistic muscle pair, the hardness measured at a single point on the skin surface cannot

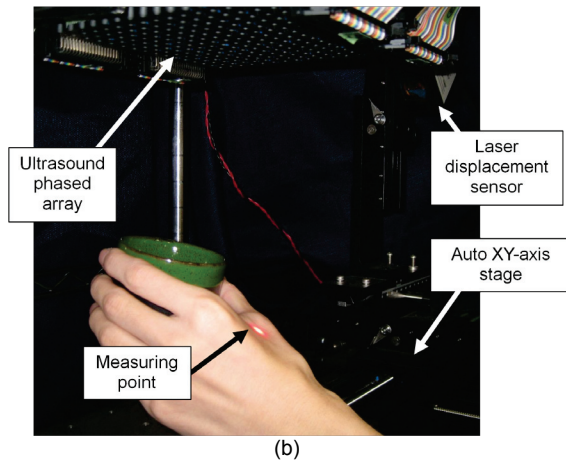
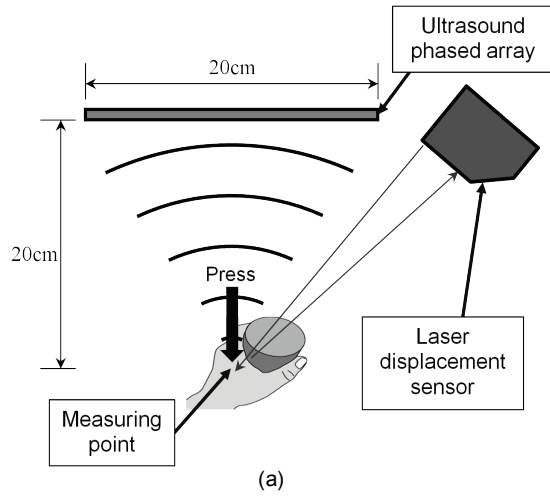


Figure 2. (a) Experimental setup of the surface hardness measurement system. (b) Appearance of the experimental setup.

determine the total force. It is difficult to estimate each muscle tension if multiple muscles exist under the hardness measurement area. Muscle fatigue and circulatory disturbance also causes muscle hardening. Nevertheless, the measurement is still useful for recording the timing when he/she strengthens the force.

## 2 NONCONTACT HARDNESS MEASUREMENT FOR GRIP FORCE CAPTURING

The measured hardness is defined in this paper as the ratio of vertical force applied to a spot circle area on an object surface to vertical displacement at its center. And corresponding compliance is the reciprocal of the hardness. The hardness and the compliance defined like this depend on the area and its shape of the applied force distribution. Supposing a virtual situation that a human finger pushes the surface, we choose about 1cm diameter circle pushed area as our previous work [8].

Our method is a direct method which presses the target surface and measures the displacement caused by the pressurization. The implemented system is composed of an airborne ultrasound phased array and a laser displacement sensor (LK-G80, Keyence corp., Japan) based on triangulation principle as shown in Figure 2. The hardness distribution is obtained by scanning the measuring

point on the surface: the pressing point and the displacement sensing point. The laser displacement sensor is moved by an auto XY-axis mechanical stage (SGSP(CS)26-200(X), SIGMA KOKI CO., LTD., Japan) and thus the measuring time is limited by the stage moving time.

### 2.1 Acoustic Radiation Pressure

Acoustic radiation pressure is non-linear phenomenon of large amplitude ultrasound [14][15]. In linear acoustics, the time average of sound pressure is zero due to symmetrical expansion and compression rate of air. As amplitude becomes larger, those rates become asymmetry due to non-linearity of air elasticity. Thus the average of sound pressure increases and this non-zero bias pressure is called acoustic radiation pressure. Assuming vertical incident on an object surface, magnitude of the acoustic radiation pressure  $P$  is represented as

$$P = (1 + R^2) \frac{p_0^2}{\rho c^2} \quad (1)$$

where  $R$  is the amplitude reflection coefficient at the object surface, and  $\rho$  is the medium density,  $c$  is the sound speed, and  $p_0$  is the RMS sound pressure of ultrasound. By utilizing the acoustic radiation pressure, it is possible to press a target surface from a remote position. Unlike pressing by an air flow, it is easy to press a small spot area on a target surface by using a converging ultrasound beam.

### 2.2 Spot Pressurization by Ultrasound Phased Array

We employ an ultrasound phased array for generating the converging ultrasound beam to press a local area on a target surface. By controlling driving phases of ultrasound transducers on the phased array so that each wave phase coincides at one point in space, an ultrasound beam is focused on that point. Because the ultrasound amplitude at the focal point is a summation of the amplitudes from all transducers, large acoustic radiation pressure occurs on the focal point according to Eq. (1).

The diameter of the focal point is comparable to the ultrasound wave length for the sufficiently large array aperture size. So the ultrasound phased array enables to press a spot area on a surface from a remote position. The measurable area can be enlarged theoretically by using larger ultrasound phased array since the focusing distance and width range is more than the array aperture size. The pressing point by the ultrasound beam can be scanned quickly on the target surface because the focal point is updated electronically. The updating time of the focal position depends on the processing speed of the phased array control system. For the ultrasound phased array used in this research, the updating time is 0.25ms and it is limited by clock frequency of the FPGA in the system [16].

### 2.3 Frequency Selection of Modulated Pressurization

For skin hardness measurement *in vivo*, we use amplitude modulated ultrasound for pressurization to avoid the effect of particular frequency background displacement noise. Assuming linear elasticity of the target object, the displacement frequency is equal to the modulation frequency. The compliance can be estimated as the ratio of displacement amplitude to the applied force amplitude at arbitrary frequency in the low frequency range of flat frequency response. We extract the displacement amplitude at the pressurization frequency from the measured displacement time series.

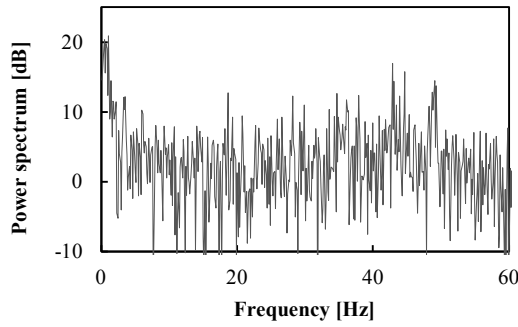


Figure 3. Background displacement noise of a static soft tissue.

Measurement accuracy per unit measurement time is inversely proportional to the band noise RMS. Thus by modulating the ultrasound amplitude at low noise rate frequency, accurate measurement can be performed in a short time. The modulation frequency is chosen considering both the power spectrum of the background displacement noise and the frequency response of the measured object. As shown in Figure 3, 0~5Hz and 42~50Hz frequency components are about 10dB larger than other range in this experimental setup. The band noise is typically low at high frequency. On the other hand, the amplitude response of a viscoelastic material for amplitude modulated pressurization decreases at high frequency in general. Thus an appropriate modulation frequency should be chosen by considering background displacement noise and the frequency response of the measured object. In this paper, we choose 40Hz as measurement frequency due to the low noise power and to the flat amplitude response of the human skin up to that frequency.

### 3 EXPERIMENTS AND RESULTS

We perform two preliminary experiments and two grip force measurement experiments to confirm the feasibility of the proposed method. First, we confirm the ability of measuring hardness change in a deep part because muscle tissue is usually covered by cutaneous membrane and subcutaneous layer. Second, we examine the measurable surface angle for measuring hardness of a curved surface. Third, a distributed surface hardness distribution of a hand which reflects muscle contraction is measured for grasping action. At last the relationship between the surface compliance and the load applied to the index finger is clarified for estimation of the grip force. As a fundamental evaluation, the situation is limited to a particular grip form by the fixed measurement system in these experiments.

#### 3.1 Experimental Setup

The proposed remote hardness measurement system is composed of the airborne ultrasound phased array and a laser displacement sensor as shown in Figure 2. This phased array is the identical to the one developed in [16]. Ultrasound transducers are arranged in a  $20\text{cm} \times 20\text{cm}$  substrate and transmit 40kHz ultrasound. The output force at the focal point is about 15mN at 20cm distant from the array. Thus, the measurable distance range is more than 20cm and the minimal focal size is about 8.5mm, which is the wave length of the 40kHz ultrasound in the air of normal temperature. The pushed spot area size is almost equal to the focal size. A measurement sample is located 20cm distant from the phased array.

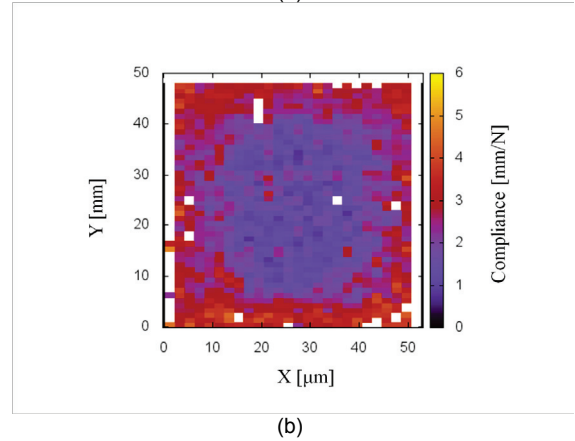
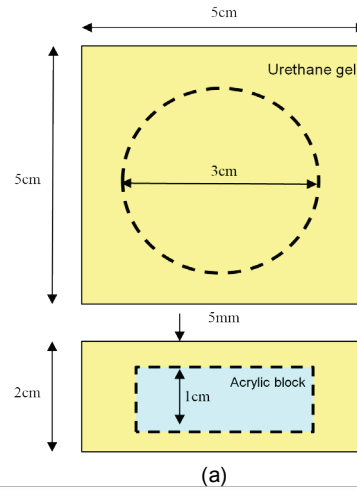


Figure 4. (a)Schematic diagram of a urethane gel sample (b) Surface hardness distribution measurement result of the sample

#### 3.2 Hardness Measurement in Deep Part

Thickness of the cutaneous membrane is almost 1~2mm, and the thickness of the subcutaneous layer strongly depends on the position. We supposed comparatively thin ( $< 3\text{mm}$ ) subcutaneous layer and examined the hardness measurement performance by a flat surface urethane gel sample (Exseal corp., Japan) with an embedded acrylic block to a depth of 5mm. The displacement at each point was measured for 0.1sec at 100Hz sampling rate. As shown in Figure 4, the hardness distribution of the acrylic block shape is blurred but the hardness difference is successfully measured.

#### 3.3 Hardness Measurement of a Curved Surface

It is necessary to correct measured compliance value for a curved surface because the acoustic radiation pressure and the measured displacement are affected by the inclined surface. We have examined such surface angle dependency of our method in [17]. The measured compliance is corrected by this dependency and [17] concludes that the correctable angle is less than 30deg. The correctable angle range is confirmed by an experiment using a molded urethane gel sample as shown in Figure 5. The experimental result is shown in Figure 6. The distance between the phased array and the measured plane is 15cm. The normal surface compliance, whose surface angle is 0, is 1.14mm/N and

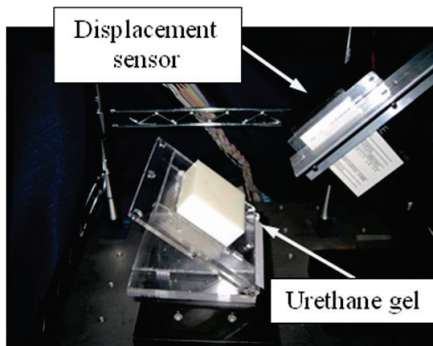


Figure 5. Appearance of an experiment which examines the measurable surface angle.

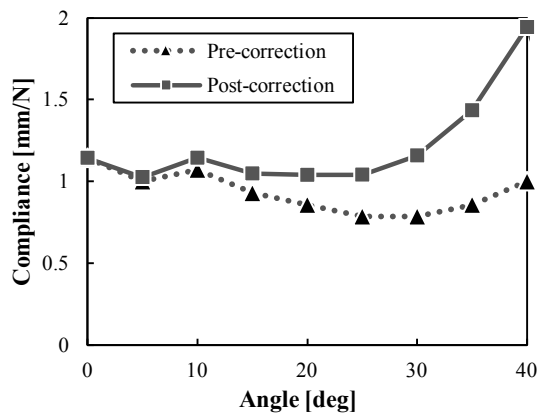


Figure 6. Correction result of surface compliance for the object surface gradient.

the value should be obtained for arbitrary surface angles, after correction. The measured surface compliance before correction is largely deviated for the angle more than 15deg. On the other hand, the corrected surface compliance maintains constant within 10% error up to the angle of 30deg.

### 3.4 Measurement of Muscle Contraction

The surface hardness measurement of skin *in vivo* is performed to confirm sensing performance of the muscle contraction. We measure the surface hardness of the left hand shown in Figure 7, while grasping action of a 6cm width rigid object. The measuring points are composed of about 1cm interval  $3 \times 3$  lattice points which are reflecting internal structure such as bones or differences of muscle thickness. These points are above the muscle between the bases of the thumb and the index finger of the left hand or above the bone. The former points are largely change the hardness for the grasping and the latter points are harder regardless of the muscle contraction. On the former points, it is expected that 40Hz vibration displacement amplitude decreases when the muscle contraction occurs.

In Figure 8, it is observed that the measured displacement contains the 40Hz vibration component of about  $25\mu\text{m}$  amplitude with slow and large fluctuation on the point of  $(X, Y) = (0, 0)$  in a relaxation state. The power spectrum of the displacement for 4.095sec of 1kHz sampling rate indicates that 40Hz component is remarkably high (32.9dB) as shown in Figure 9. Besides, 120Hz, 200Hz, and 280Hz components are also observed since these odd-

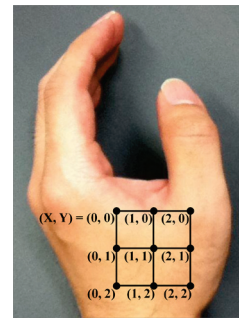


Figure 7. Surface hardness measuring points on the left hand for the contraction measurement experiment.

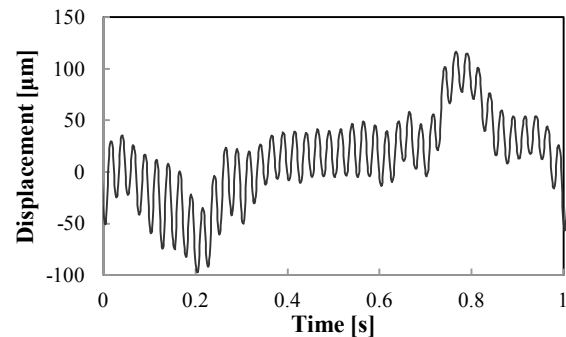


Figure 8. Measured displacement at  $(X, Y) = (0, 0)$  in a relaxation state.

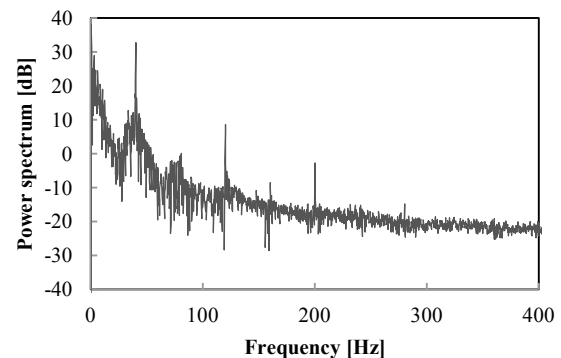


Figure 9. Power spectrum of the displacement at  $(X, Y) = (0, 0)$  in a relaxation state.

order components are included in the 40Hz square wave. The large fluctuation noise is gathered in the low frequency band when the hand position is fixed.

As shown in Figure 10, for a contracted state, the measured displacement does not contain 40Hz vibration component. As Figure 11 shows, the power of 40Hz component is 8.58dB that is 24.3dB smaller than the value for the relaxation state. Those are easily discriminated using the measured displacement time series.

The measured compliance distribution for the contraction and relaxation state is represented in Figure 12. For the contraction state, the compliances on the whole point are close to or lower than those of the relaxation state. For the relaxation state, the points of  $(X, Y) = (1, 0)$ ,  $(0, 0)$ , and  $(0, 1)$  have significantly high compliances than those of contraction state. On the other hand, the

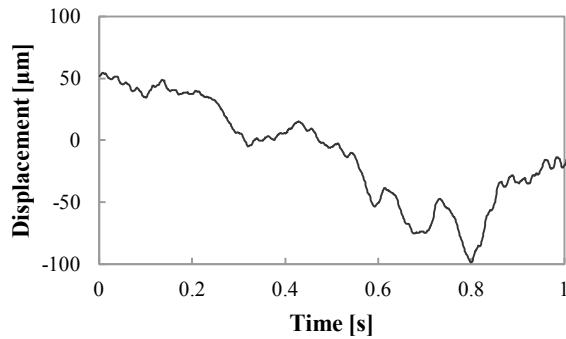


Figure 10. Measured displacement at  $(X, Y) = (0, 0)$  in a contraction state.

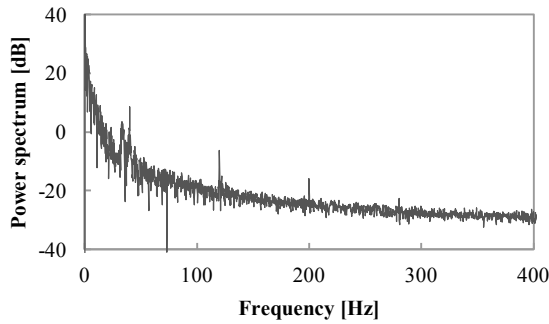


Figure 11. Power spectrum of the displacement at  $(X, Y) = (0, 0)$  in a contraction state.

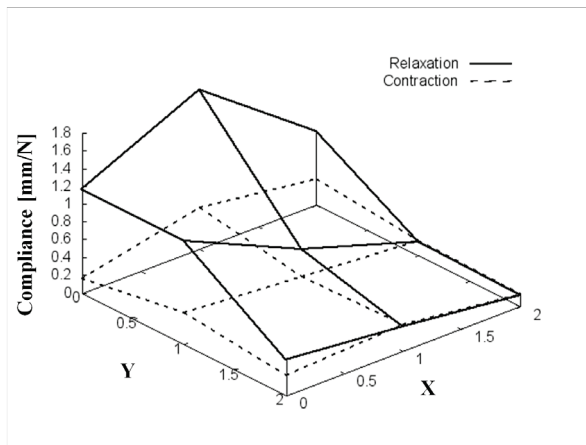


Figure 12. Measured compliance distribution on the skin surface in Figure 7.

compliances on the points of  $(X, Y) = (0, 2), (1, 2), (2, 2),$  and  $(2, 1)$  have low values regardless of the state because those points are above the hard and undeformable bone.

### 3.5 Relationship between Surface Compliance and Grip Force

The time series of the surface compliance of the measured displacement at the point  $(X, Y) = (0, 0)$  for continuous grasping action is shown in Figure 13. The displacement, which is measured for 8.192sec at 1kHz sampling rate, is divided into every 128ms and 512ms interval. Each 40Hz vibration component

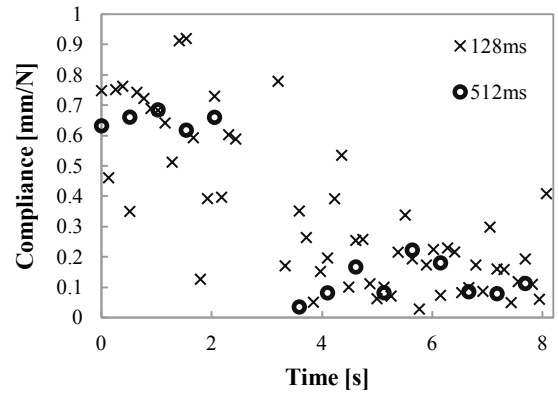


Figure 13. The measured compliance time series at  $(X, Y) = (0, 0)$  in a grasping action

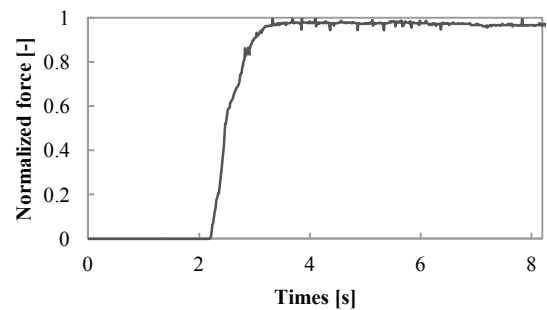


Figure 14. Grip force transition measured by a force sensor mounted on the grasped object

is calculated from each interval. Grasping timing is represented in Figure 14 where the grip force was measured with a pressure sensor mounted on the object. In Figure 13, the measured compliance for 512ms sampling rate is larger than 0.6mm/N in the range of the zero force phase, and is less than 0.2mm/N in the range of the gripping phase. Therefore the discrimination between the relaxation and contraction state can be achieved in continuous grasping action at intervals of about 500ms. On the other hand, the compliance series for the 128ms intervals are noisier. The 40Hz component fluctuates temporally during the force transition interval because the skin surface vibrates by the intentional action.

For grip force estimation, the relationship between the grip force and the surface compliance of skin are measured. Figure 15(a) shows a measuring point of the compliance and the loading point. The hand posture is kept through the experiment for measuring the isotonic contraction. The measured relationship is shown in Figure 15(b). The displacement is measured at 1kHz sampling rate for 1.024sec for 40Hz modulated pressurization and the error bars indicate the standard deviation of eight measurements. The compliance decreases monotonically with the increase of the load.

## 4 CONCLUSIONS AND FUTURE WORK

In this paper, we proposed a remote grip force sensing method based on skin surface hardness measurement. The surface hardness of the hand increases with grasping force. The change of skin surface hardness was measured by a system which consisted of an airborne ultrasound phased array and a laser displacement

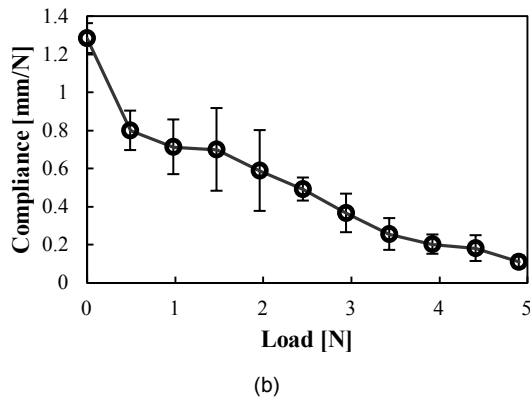
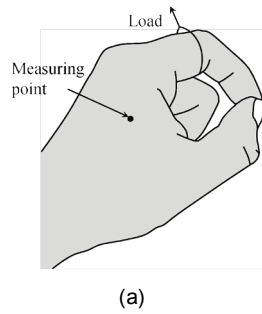


Figure 15. (a) A measuring point and a loading point on the hand. (b) Measured relationship between the surface compliance and the load

sensor. The hardness distribution of a human hand was measured for contracted and relaxed states. The muscle hardness change between the contraction and relaxation state was observed for 512ms period measurement using 40Hz amplitude modulated pressurization. In the isometric contraction, the relationship between the hand compliance and the grip force were clarified up to 5kN load. The future work is real-time hardness distribution measurement in motion for more general grasping ways by noise reduction based on the signal/noise and temporal/spatial properties. It is also a challenge to estimate the actual force from obtained hardness distribution in general situations considering inter-subject factors.

## REFERENCES

- [1] G. J. Tortora and B. Derrickson. *Principles of Anatomy and Physiology (11<sup>th</sup> edition)*. John Wiley & Sons, 2005.
- [2] J. H. Lawrence and C. J. De Luca. Myoelectric signal versus force relationship in different human muscles. *Journal of Applied Physiology*, Volume 54, Number 6, pages 1653-1659, June 1983.
- [3] P. A. Tesch, G. A. Dudley, M. R. Duvoisin, B. M. Hather, and R. T. Harris. Force and EMG signal patterns during repeated bouts of concentric or eccentric muscle actions. *Acta Physiologica Scandinavica*, Volume 138, Issue 3, pages 263-271, March 1990.
- [4] L. Arendt-Nielsen and K.R Mills. The relationship between mean power frequency of the EMG spectrum and muscle fibre conduction velocity. *Electroencephalography and Clinical Neurophysiology*, Volume 60, Issue 2, pages 130-134, February 1985.
- [5] L. Arendt-Nielsen, K.R Mills, and A. Forster. Changes in muscle fiber conduction velocity, mean power frequency, and mean EMG voltage during prolonged submaximal contractions. *Muscle & Nerve*, Volume 12, Issue 6, pages 493-497, June 1989.
- [6] S. H. Westing, A. G. Cresswell, and A. Thorstensson, Muscle

- activation during maximal voluntary eccentric and concentric knee extension. *European Journal of Applied Physiology and Occupational Physiology*, Volume 62, Issue 2, pages 104-108, 1991.
- [7] P. V. Komi, V. Linnamo, P. Silventoinen, and M. Sillanpää. Force and EMG power spectrum during eccentric and concentric actions. *Medicine and science in sports and exercise*, Volume 32, Issue 10, pages 1757-1762, 2000.
- [8] M. Fujiwara, K. Nakatsuma, M. Takahashi, and H. Shinoda. Remote Measurement of Surface Compliance Distribution Using Ultrasound Radiation Pressure. In *Proc. of IEEE World Haptics Conference 2011*, pages 43-47, 2011.
- [9] M. Murayama, K. Watanabe, R. Kato, T. Uchiyama, and T. Yoneda. Association of muscle hardness with muscle tension dynamics: a physiological property. *European Journal of Applied Physiology*, Volume 112, Number 1, pages 105-112, 2012.
- [10] M. Ashina, L. Bendtsen, R. Jensen, F. Sakai, and J. Olesen. Measurement of muscle hardness: a methodological study. *Cephalalgia*, Volume 18, Issue 2, pages 106-111, March 1998.s
- [11] T. Sugimoto, S. Ueha, and K. Itoh. Tissue hardness measurement using the radiation force of focused ultrasound. *Proc. of Ultrasonics Symposium*, Volume. 3, pages 1377-1380, December 1990.
- [12] K. Nightingale, M. S. Soo, R. Nightingale, and G. Trahey. Acoustic radiation force impulse imaging: in vivo demonstration of clinical feasibility. *Ultrasound in Medicine & Biology*, Volume 28, Issue 2, pages 227-235, February 2002.
- [13] J. F. Greenleaf, M. Fatemi, and M. Insana. Selected methods for imaging elastic properties of biological tissues. *Biomedical Engineering*, Volume 5, pages 57-78, April 2003.
- [14] J. Awatani. Studies on Acoustic Radiation Pressure. I. (General Considerations). *Journal of the Acoustical Society of America*, Volume 27, pages 278-281, 1955.
- [15] T. Hasegawa, T. Kido, T. Iizuka, and C. Matsuoka. A General Theory of Rayleigh and Langevin Radiation Pressures. *Acoustical Science and Technology*, Volume 21, Number 3, pages 145-152, 2000.
- [16] T. Hoshi, M. Takahashi, T. Iwamoto, H. Shinoda. Non-contact Tactile Display Based on Radiation Pressure of Airborne Ultrasound. *IEEE Transactions on Haptics*, Volume 3, Number 3, pages 155-165, 2010.
- [17] M. Fujiwara and H. Shinoda. Remote Measurement Method of Surface Compliance Distribution for a Curved Surface Object. In *Proc. of SICE Annual Conference 2012*, pages 1-5, Akita, Japan, August 2012.